Synthesis and Reactivity at the Ir-^{Me}Tpm Platform: From κ^1-*N* Coordination to κ^3–N- based Organometallic Chemistry.

Francisco J. Fernández-Alvarez,[a] Víctor Polo,[b] Pilar García-Orduña,[a] Fernando J. Lahoz,[a] Jesús J. Pérez-Torrente,[a] Luis A. Oro[a] and Ralte Lalrempuia*[a,c]

Reaction of [Ir(μ-Cl)(COE)$_2$]$_2$ (COE = *cis*-cyclooctene) with tris(3,5-dimethylpyrazol-1-yl)methane (^{Me}Tpm) affords [IrCl(κ^1-*N*-^{Me}Tpm)(COD)] (**1**) (COD = 1,5-cyclooctadiene). The formation of **1** implies the transfer dehydrogenation of a COE ligand to give COD and COA (cyclooctane). A mechanistic proposal based on DFT calculations that explains this iridium promoted process has been disclosed. Additionally, reactivity studies have allowed the preparation and characterization, including determination of the molecular structures of a number of iridium complexes with the ^{Me}Tpm ligand in κ^1, κ^2 or κ^3-*N* coordination modes. Moreover, the first example of an Ir-cyclooctyl complex featuring hydride and carbonyl ligands, whose solid state structure has been determined by X-ray diffraction methods, is reported.

Introduction

The neutral tris(pyrazolyl)methanes (HC(R$_2$pz)$_3$, ^{R}Tpm)[1] and the related anionic tripodal ligands, tris(pyrazolyl)hydroborates (HB(R$_2$pz)$_3$, ^{R}Tp),[2] possess pyrazolyl-based lone pairs, allowing coordination of metals across the periodic table. The metallation chemistry of these classes of ligand is largely dominated by κ^2-*N* and κ^3-*N* ligation (**A** and **B**, Chart 1), few examples of bonding mode **C** are known[3] and one example exist for the type **D** [4]. While few metal complexes with ^{R}Tp in κ^1-*N* coordination mode have been already described,[5] the monodentate coordination mode (**E**, Chart 1) is so far unknown for the ^{R}Tpm ligands.

While the chemistry of iridium complexes with anionic ^{R}Tp ligands has been widely and successfully explored,[2b,2c,2d,3] the chemical behaviour of Ir-^{R}Tpm species has been only scarcely studied.[6] This may be due to comparatively much less focus on the coordination chemistry of the neutral ^{R}Tpm ligands. Penta-coordinated rhodium and iridium [MCl(κ^2-^{H}Tpm)(diolefin)] and [M(κ^3-^{H}Tpm)(diolefin)]Cl (M = Rh, Ir) complexes have been prepared by reaction of the corresponding chloro-bridged metallic precursor with the stoichiometric amount of the ^{H}Tpm ligand.[6f]

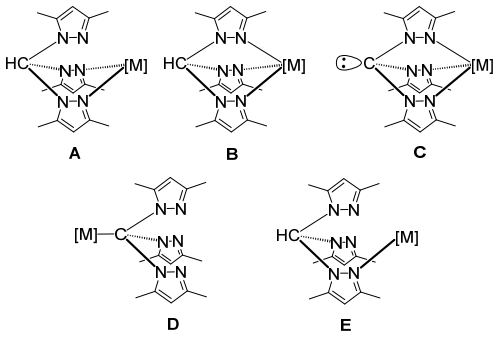

Chart 1. Known coordination mode of ^{R}Tpm

Herein, we report on the synthesis of κ^1-*N* ligated ^{R}Tpm species, [IrCl(κ^1-*N*-^{Me}Tpm)(COD)] (**1**) (COD = 1,5-cyclooctadiene) and the subsequent reactivity studies showing sequential denticity variation of the tris(3,5-dimethylpyrazol-1-yl)methane (^{Me}Tpm) ligand from κ^1-*N* to κ^2-*N,N´* and κ^3-*N,N´,N´´* coordination modes. To the best of our knowledge complex **1** is the first example of a transition metal complex with a ^{R}Tpm ligand in κ^1-*N* coordination mode. The formation of complex **1** featuring a COD ligand starting from [Ir(μ-Cl)(COE)$_2$]$_2$ (COE = *cis*-cyclooctene) and ^{Me}Tpm also prompted us to undertake a theoretical and experimental study on the mechanism of this Ir-^{Me}Tpm promoted COE dehydrogenation reaction.

RESULTS AND DISCUSSION

Reactivity of ^{Me}Tpm with [Ir(μ-Cl)(COE)$_2$]$_2$.

To shed light on the reactivity pattern of ^{Me}Tpm with [Ir(μ-Cl)(COE)$_2$], we decided to monitor the reaction with ^{1}H NMR spectroscopy. ^{1}H NMR studies of the reaction of [Ir(μ-Cl)(COE)$_2$]$_2$ with ^{Me}Tpm at 298 K showed no reaction in CD_2Cl_2 and a very slow reaction in C_6D_6. However, after heating the samples prepared in C_6D_6 at 353 K the formation of [IrCl(κ^1-*N*-^{Me}Tpm)(COD)] (**1**) (80 % based on ^{1}H NMR integration) was observed after one hour. Complete conversion of the starting iridium precursor was achieved in 24 h to afford complex **1** and the stoichiometric amount of cyclooctane (COA), which was identified by ^{1}H and ^{13}C{^{1}H} NMR spectroscopy.[7] The presence of traces of free COE and Ir-hydride containing species was also observed during the reaction. The routine work up of the C_6D_6 solution afforded **1** as greenish-yellow powder. With the aim to disclose a direct synthetic methodology to obtain **1**, the reaction of ^{Me}Tpm with [Ir(μ-Cl)(COD)]$_2$ in toluene at room temperature was investigated. This procedure allows quantitative formation of complex **1** within 2 h (Scheme 1).

^{1}H NMR spectrum of complex **1** at room temperature shows broad signals, although a more defined spectrum was observed at 193 K, which is in agreement with the dynamic behaviour described for related Ir-^{H}Tpm species.[6f] The ^{1}H NMR spectra of **1** in CD_2Cl_2 at 193 K shows three resonances for the pyrazolyl-CH protons at δ 6.07, 6.03 and 5.88 ppm, which evidenced the inequivalence of the three pyrazolyl rings. The resonance corresponding to the methine proton is observed as a singlet at

[a] *Departamento de Química Inorgánica-Instituto de Síntesis Química y Catálisis Homogénea (ISQCH), Universidad de Zaragoza–CSIC, Facultad de Ciencias 50009, Zaragoza, Spain.*
[b] *Departamento de Química Física-Instituto de Biocomputación y Física de Sistemas Complejos (BIFI), Universidad de Zaragoza–CSIC, Facultad de Ciencias 50009, Zaragoza, Spain.*
[c] *School of Chemical Sciences, Dublin City University, Dublin 9, Ireland; e-mail: lalrempuia.ralte@dcu.ie*

DOI 10.1039/c9dt00703b

δ 9.15 ppm, low-field shifted in comparison with the related resonance for the free ^{Me}Tpm ligand (δ 7.98 ppm). The remaining ^{1}H and ^{13}C NMR resonances agree with the structure proposed for **1** in Scheme 1 (see Experimental Section).

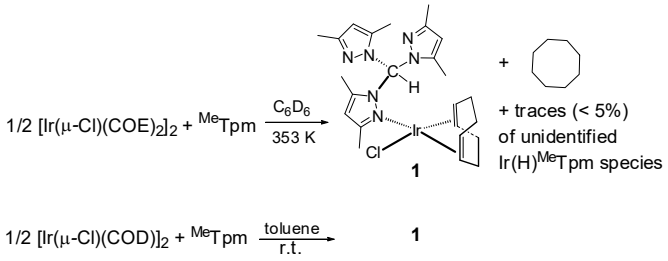

Scheme 1. Reactivity of dinuclear Ir(I) precursors with tris(3,5-dimethylpyrazol-1-yl)methane.

Complex **1** has been unambiguously characterized by elemental analysis, ^{1}H and ^{13}C NMR spectroscopy and by X-ray diffraction. Greenish yellow coloured single crystals of **1** were obtained from a saturated benzene solution. Complex **1** crystallizes with two crystallographically independent but structurally similar and chemically identical molecules in the asymmetric unit (Figure S1, ESI). Selected structural parameters are summarized in Table 1. Iridium atoms exhibit slightly distorted square-planar geometries with the coordination of a chloride and a COD ligand in its η^4- usual bonding mode and the Ir-κ^1-N ligation of the ^{Me}Tpm ligand through one of the nitrogen atom to the Ir(I) center (Figure 1). A 2.115(2) Å Ir-N bond length has been found in this new-fangled coordination of ^{Me}Tpm fragment, very close to those reported for related Ir-N bond *trans* to olefins in Ir-(κ^2-*N,N´*-^{Me}Tpm) (2.111(3) and 2.112(3) Å)[6b] and Ir-(κ^3-*N,N´,N´´*-^{Me}Tpm) (2.104(5) Å)[6c] fragments. Significantly longer distances (5.770(2) and 4.530(2) Å) are found between Ir and N(3) and N(5) nitrogen atoms of the uncoordinated pyrazole groups. Uncoordinated pyrazolyl groups in complex **1** are oriented away from the metal center. Dihedral angles in the range (66.22(1)–88.19(11)°) are found between the pyrazolyl mean planes (Table S1, ESI). Tetrahedral geometry of the C(6) apical carbon atom of the ligand exhibits similar C-N bond lengths and N-C-N angles with 1.449(2)Å and 111.08(8)° mean values. Although H(6) proton is oriented towards the metal, the 2.74(3) Å Ir···H distance excludes the existence of an agostic interaction, which is in agreement with the observed in related κ^1-*N*-^{R}Tp coordinated transition metal complexes.[5a,8] In fact, the existence of a loose agostic interaction had only been suggested in [Rh($^{Me2,4-Cl}$Tp)(CO)(PMePh$_2$)$_2$] complex where the apical hydrogen atom is located in the potential axial metal site, with a Rh···H distance of 2.35(3) Å.[9]

The ability of iridium complexes to catalyze the transfer dehydrogenation of alkanes has been well documented during the last decades.[10] The formation of **1** and COA from the reaction of [Ir(μ-Cl)(COE)$_2$]$_2$ with ^{Me}Tpm constitutes an example of transfer dehydrogenation of COE to afford COD, with simultaneous hydrogenation of the second COE molecule to COA. In this context, it should be mentioned that a few examples of iridium promoted dehydrogenation of COE to COD have been reported.[11]

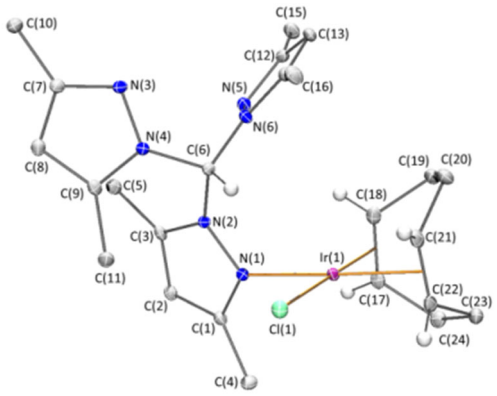

Figure 1. Molecular structure of one of the crystallographically independent molecules of **1**. For clarity, most of the hydrogen atoms have been omitted.

Iridium-promoted C-H bond activation of the allylic hydrogens of the COE ligand to afford 1,3-COD[12] and subsequent isomerization involving insertion, and ß-hydrogen elimination elementary steps sequences has been proposed to explain the transfer dehydrogenation of COE to give 1,5-COD.[13] In this context, mechanistic and experimental studies supporting the facile and reversible iridium-promoted exchange of hydrogens between Ir-H and COD ligand have been reported.[13] However, based on the experimental evidence reported by Crabtree et al., the direct attack of the iridium centre to unactivated C-H bonds of the COE ligand cannot be ruled out.[14] The lack of knowledge on the mechanism of such transformation motivated us to study the reaction by NMR spectroscopy and to perform theoretical calculations at the DFT level on the model complex [IrCl(κ^1-*N*-^{Me}Tpm)(COE)$_2$].

Figure 2 shows the mechanistic proposal for both dehydrogenation (red path) and hydrogenation (blue path) of COE. The reaction starts by the dissociation of one COE molecule, which has been corroborated by ^{1}H NMR, followed by oxidative addition of one of the unactivated C^5-H bonds of the COE ligand to the iridium(I) center (red path) via transition state **TSBC** (12.5 kcal mol^{-1}) leading to the Ir(III) intermediate **C** in a slightly exergonic step (-3.0 kcal mol^{-1}). The alternative route via oxidative addition of one of the activated C^3-H bonds of the COE ligand requires to overcome a higher energy barrier (**TSBC´**, 15.5 kcal mol^{-1}) to give the Ir-allylic intermediate **C´**. This activation process is endergonic by 5.4 kcal mol^{-1} (Figure S9, ESI).

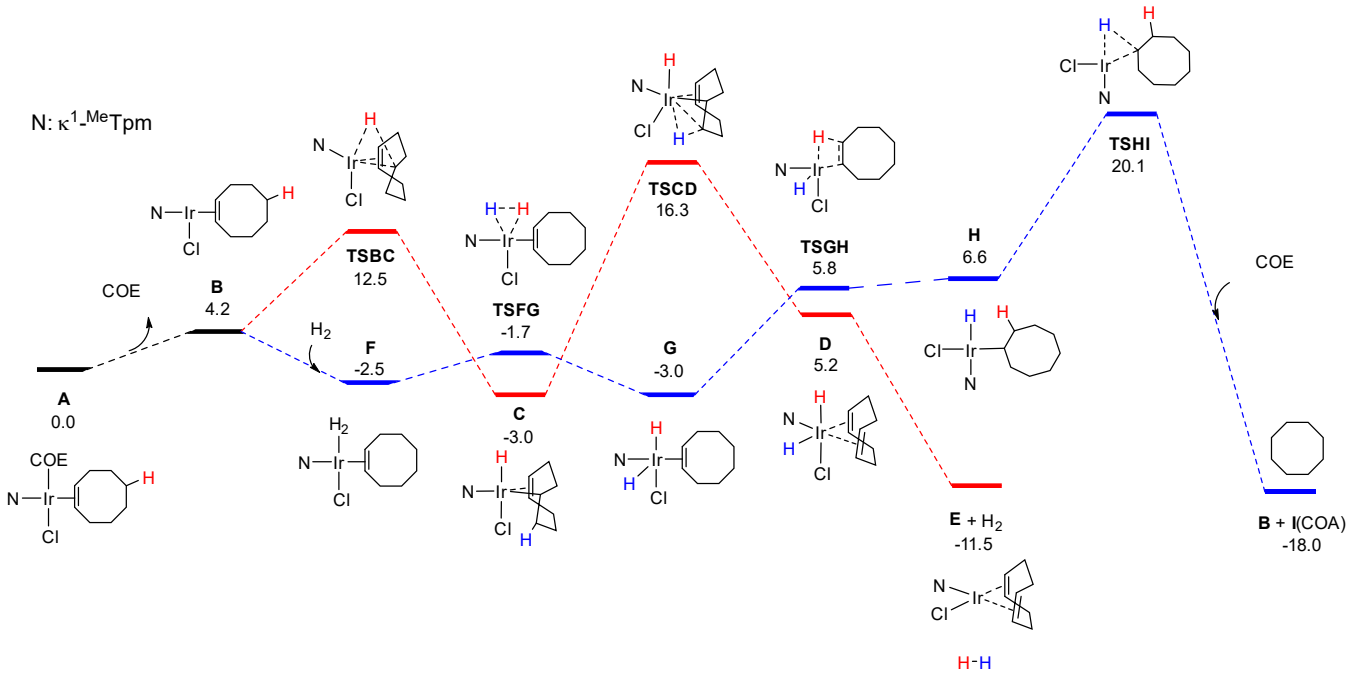

Figure 2. DFT calculated Gibbs free energy profile (in kcal mol^{-1}, respect to **A**), for the iridium-promoted dehydrogenation (red path) and hydrogenation (blue path) of COE from [IrCl(κ^1-*N*-^{Me}Tpm)(COE)$_2$] (**A**).

Therefore, the mechanism via C^5-H bond activation represents a feasible mechanistic option. Moreover, an iridium complex with an Ir-κ^1-4,5-η-cyclooctenyl moiety analogous to the intermediate species **C** has been reported by some of us.[15] The dihydride intermediate **D** is formed from **C** by β-hydrogen elimination through the transition state **TSCD**. This step corresponds to the higher energy barrier of the overall dehydrogenation process (19.3 kcal mol^{-1}). Finally, complex **E** is formed by dihydrogen reductive elimination from **D**, being the overall process exergonic by -11.5 kcal mol^{-1}. The hydrogen molecule generated in the above described process (red path) could coordinate to the metal in **B** to yield intermediate **F** (blue path). The oxidative addition of H_2 to the metal takes place via a low energy barrier, characterized by transition state **TSFG**, forming the dihydride intermediate **G**. Hydrogenation of COE takes places via 1,2-migratory insertion of the olefin into the Ir-H bond (**TSGH**) followed by reductive elimination of COA through **TSHI**. The last step shows the higher energetic barrier for the overall hydrogenation process (23.1 kcal/mol^{-1}). An analogous mechanistic proposal, involving consecutive β-hydrogen elimination and olefin insertion, has been recently reported for explaining the transformation of the cationic complex [Ir(η^3-cyclooctenyl){κ^3-*S,Si,S*-(SiMe{*o*-C$_6$H$_4$SMe$_2$}$_2$}]$^+$ into the [Ir(COD)(H){κ^3-*S,Si,S*-(SiMe{*o*-C$_6$H$_4$SMe$_2$}$_2$}]$^+$ species.[16]

Reactivity of complex [IrCl(κ^1-*N*-^{Me}Tpm)(COD)] (1).

The unusual κ^1-N ligation mode of the ^{Me}Tpm in complex **1** calls for further reactivity studies. Thus, treatment of complex **1** with an halide scavenger, AgOTf (OTf = $CF_3SO_3^-$) in CH_2Cl_2 resulted in the release of AgCl, affording a κ^2-*N* ligated cationic iridium(I) complex, [Ir(κ^2-*N,N'*-^{Me}Tpm)(COD)]OTf (**2.OTf**), which could be isolated in quantitative yield (Scheme 2). This air stable orange-red solid was initially identified by comparison of its ^{1}H and ^{13}C{^{1}H} NMR spectra with those of the reported **2·PF$_6$** salt.[6b] The most noticeable feature in the ^{1}H NMR spectrum of **2·OTf** in CD_2Cl_2 is a significant up-field shift of the resonance corresponding to the bridged C-H group, from δ 9.15 (**1**) to δ 7.83 (**2·OTf**) ppm. It must be noted here that the ^{1}H NMR recorded at room temperature and 193 K showed no significant difference (See ESI, Figure S4 and S5). The molecular structure of **2·OTf** has been determined by an X-ray diffraction study (Figure 3).

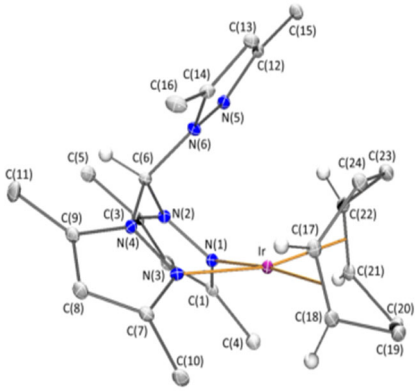

Figure 3. Molecular structure of the cation of **2·OTf**. For clarity, most of the hydrogen atoms have been omitted.

The solid state structure of complex **2·OTf** shows the metal atom in a slightly distorted square planar environment, with N(1)-Ir-Ct(1) and N(3)-Ir-Ct(2) *trans* angles significantly deviating from 180° value (174.61(8) and 167.90(8)°, respectively) due to the bidentate coordination of both ligands. The carbocyclic ligand is coordinated in its usual η^4-coordination

mode while the ^{Me}Tpm fragment is found to be κ^2-N coordinated through two nitrogen atoms. No statistically significant difference is shown between both Ir-N bond lengths. Moreover, these values are close to that found in complex **1** (Table 1). The uncoordinated pyrazole ring is oriented in the axial position of the apical C(6) carbon atom, pseudo-parallel to the iridium coordination mean plane, establishing with it a 47.51(6)° dihedral angle. This disposition leads to an intramolecular Ir-N_{apical} distance of 3.602(2) Å. This geometrical arrangement is close to that found in complex [Rh(CO)(PPh_3)(κ^2-*N*-^{Me}Tpm)][PF_6].[17]

Table 1. Selected bond lengths (Å) and angles (°) for molecular structure of compounds **1** and **2·OTf**.

	1a[a]	**1b**[a]	**2·OTf**
Ir-Cl	2.3449(7)	2.3429(8)	-
Ir(1)-N(1)	2.115(2)	2.117(3)	2.1172(18)
Ir(1)-N(3)	-	-	2.1101(17)
Ir(1)-Ct(1)[b]	1.988(3)	1.988(3)	2.014(2)
Ir(1)-Ct(2)[b]	2.008(3)	2.006(3)	2.007(2)
Cl(1)-Ir(1)-N(1)	89.80(7)	89.03(7)	-
Cl(1)-Ir(1)-Ct(1)[b]	179.27(9)	177.91(9)	-
Cl(1)-Ir(1)-Ct(2)[b]	91.22(9)	90.45(9)	-
N(1)-Ir-N(3)	-	-	82.40(7)
N(1)-Ir(1)-Ct(1)[b]	90.88(11)	92.85(11)	174.61(8)
N(1)-Ir(1)-Ct(2)[b]	178.28(11)	177.79(11)	95.86(8)
N(3)-Ir(1)-Ct(1)[b]	-	-	96.10(8)
N(3)-Ir(1)-Ct(2)[b]	-	-	167.90(8)

(a) **1a** and **1b** are the two independent molecules of **1** in the unit cell; (b) Ct are centroids of the olefinic bonds of COD ligands.

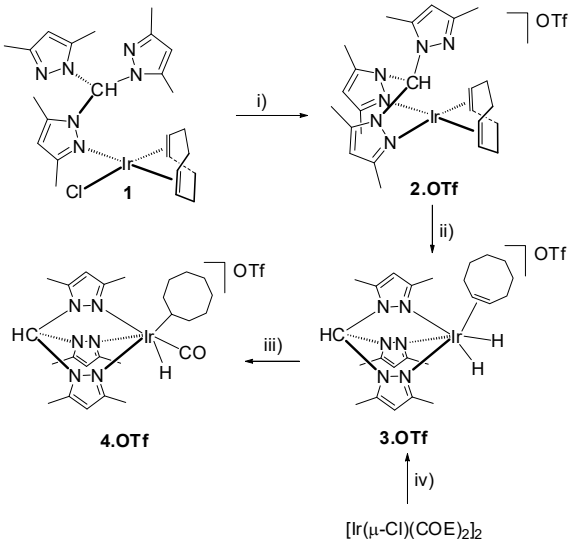

Scheme 2. Reactivity of Ir-^{Me}Tpm complexes: i) AgOTf, r.t.; ii) H_2 (2 bar), 323 K; iii) CO (2 bar), 323 K; iv) 2 ^{Me}Tpm, 2 NaOTf, H_2 (1 bar) r.t.

Keeping in mind the possible N-pendant pyrazole-metal synergistic roles in activation of small molecules such as hydrogen, we looked at the reactivity of **2·OTf** with molecular hydrogen. Indeed, **2·OTf** slowly reacts with H_2 to evolved into a κ^3-*N* ligated oxidative addition product, the Ir(III)-hydride species [IrH_2(κ^3-*N,N´,N´´*-^{Me}Tpm)(COE)]OTf (**3·OTf**). Monitoring the reaction by ^{1}H NMR did not reveal information about the reaction mechanism as the likely dihydride-cyclooctadiene intermediate was not observed.

The reaction is sluggish and requires heating at 323 K for three days. However, one pot reaction of a mixture of [Ir(μ-Cl)(COE)$_2$]$_2$, ^{Me}Tpm and NaOTf with dihydrogen (1 bar) at room temperature quantitatively affords **3·OTf** in less than one hour (Scheme 2). Complex **3·OTf** has been fully characterized by, ^{1}H and ^{13}C{^{1}H} NMR, IR, elemental analysis and by X-ray crystallography (Figure 4).

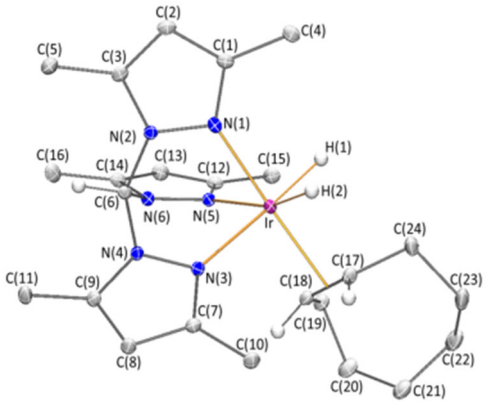

Figure 4. Molecular structure of the cation of **3·OTf**. Most hydrogen atoms have been omitted for clarity. Selected bond lengths (Å) and angles (°): Ir–N(1) 2.0747(18), Ir–N(3) 2.1957(17), Ir–N(5) 2.1786(17), Ir–Ct[a] 2.067(2), Ir–H(1) 1.629(10), Ir–H(2) 1.626(10), N(1)-Ir-N(3) 84.17(6), N(1)-Ir-N(5) 79.63(7), N(1)-Ir-Ct[a] 172.19(8), N(1)-Ir-H(1) 93.0(12), N(1)-Ir-H(2) 85.5(12), N(3)-Ir-N(5) 88.26(6), N(3)-Ir-Ct[a] 93.84(8), N(3)-Ir-H(1) 176.4(12), N(3)-Ir-H(2) 95.1(12), N(5)-Ir-Ct[a] 107.91(8), N(5)-Ir-H(1) 93.4(11), N(5)-Ir-H(2) 164.4(12), Ct[a]-Ir-H(1) 88.7(9), Ct[a]-Ir-H(2) 87.1(11), H(1)-Ir-H(2) 82.5(16), [a]Ct is the centroid of the C(17)=C(18) olefinic bond.

The most outstanding features of the ^{1}H NMR spectra of **3·OTf** are a singlet resonance for the equivalent hydride ligands and a multiplet assigned to the two olefinic protons of the η^2-COE ligand which appear at δ -22.82 and 4.12 ppm, respectively. A noticeable up-field shift trend has been observed for the methine carbon and proton resonances when shifting from κ^1-*N* to κ^2-*N,N´* and to κ^3-*N,N´,N´´* ligation. The tendency for complexes **1**, **2·OTf** and **3·OTf** is δ 78.6, 74.9, 70.6 ppm and δ 9.15, 7.83, 7.81 ppm in the ^{13}C{^{1}H} and ^{1}H NMR spectra, respectively. The IR spectra of **3·OTf** show an absorption at 2190 cm^{-1}, which is assigned to the Ir-H bonds.

Insertion of the COE ligand into one of the Ir-H bonds of **3·OTf**, can be forced by heating dichloromethane solution at 323 K under CO (2 bar) atmosphere. ^{1}H NMR monitoring of this reaction showed that the reaction need three days to fully convert to [IrH(σ-cyclooctyl)(CO)(κ^3-*N,N´,N´´*-^{Me}Tpm)]OTf (**4·OTf**) (Scheme 2). This compound was isolated as a white crystalline solid from reddish-yellow coloured reaction solution. The ^{1}H NMR spectra of **4·OTf** in CD_2Cl_2 show the resonance corresponding to the H_α of the σ-cyclooctyl ligand as a multiplet at δ 3.35 ppm, which correlates with the C-H resonance at δ 9.8 ppm in the ^{1}H-^{13}C HSQC NMR experiment. The resonance for Ir-H appears at δ –18.05 ppm. The molecular structure of **4·OTf**

has been determined by an X-ray crystallography study (Figure 5). It should be noted that the tridentate coordination mode of the ^{Me}Tpm ligand imposes a *cis* disposition of the σ-cyclooctyl, carbonyl and hydride ligands (Figure 5).

Complexes **3·OTf** (Figure 4) and **4·OTf** (Figure 5) exhibit octahedral metal coordination centers, with four sites occupied by one hydride and the ^{Me}Tpm ligand acting in its usual tridentate coordination. Remaining metal coordination sites are fulfilled by a hydride and a COE ligand in **3·OTf**, and by a carbonyl and a cyclooctyl ligands in **4·OTf**.

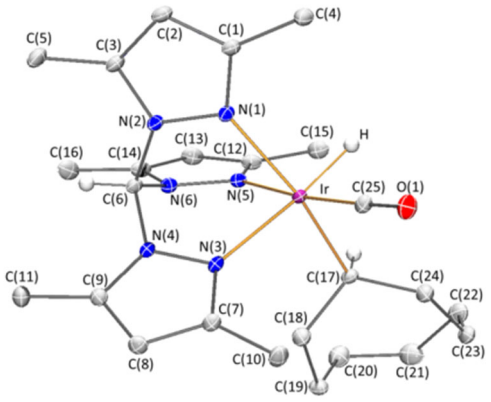

Figure 5. Molecular structure of the cation of **4·OTf**. Most hydrogen atoms have been omitted for clarity. Selected bond lengths (Å) and angles (°): Ir–N(1) 2.1935(19), Ir–N(3) 2.1631(19), Ir–N(5) 2.098(2), Ir–C(17) 2.133(2), Ir–C(25) 1.837(2), Ir–H 1.49(3), N(1)-Ir-N(3) 80.42(7), N(1)-Ir-N(5) 79.86(7), N(1)-Ir-C(17) 166.70(8), N(1)-Ir-C(25) 100.39(9), N(1)-Ir-H 93.8(10), N(3)-Ir-N(5) 89.56(7), N(3)-Ir-C(17) 95.80(8), N(3)-Ir-C(25) 96.71(9), N(3)-Ir-H 174.2(10), N(5)-Ir-C(17) 87.40(8), N(5)-Ir-C(25) 173.68(9), N(5)-Ir-H 90.2(10), C(17)-Ir-C(25) 92.69(10), C(17)-Ir-H 90.0(10), C(25)-Ir-H 83.4(10).

The N-Ir-N bond angle values are similar in both complexes and slightly deviated from the 90° ideal value, due to bite of the tridentate ligand, leading to the formation of three Ir-N-N-C-N-N metallacycles with a boat conformation (see ESI). Interestingly, **3·OTf** and **4·OTf** exhibit dissimilar Ir-N bond lengths, with one of them (namely Ir-N(1) in **3·OTf** and Ir-N(5) in **4·OTf**) being shorter than the others, reflecting the differing *trans* influence of the ligands. For instance, in **3·OTf** Ir-N(3) and Ir-N(5) bond lengths are similar (N(3) and N(5) being *trans* to strong *trans*-influencing hydride ligands) and longer than Ir-N(1). The latter is closer to the values found in **1** and **2·OTf** for N *trans* to centroid of olefinic bonds.

The Ir-carbocyclic ligand coordination in the above-mentioned complexes deserves further comments. The η^2-coordination of COE in **3·OTf** is characterized by a 2.067(2) Å distance between the metal atom and the centroid of the olefinic bond, slightly longer than those found in the Ir-COD moiety in complexes **1** and **2·OTf**, and like others Ir-η^2-COE in complexes reported by some of us.[18] The Ir-σ-cyclooctyl motif in **4·OTf** is much less common. It is noteworthy of mentioning that although Ir-σ-cyclooctyl intermediates have been proposed in COE hydrogenation processes,[11b,19] only few examples of such species have been reported.[20] In addition, to the best of our knowledge none of them have been structurally characterized. Carbon-carbon bond lengths in the 1.516(4)-1.539(2) Å range have been observed in the carbocyclic ligand in **4·OTf**, precluding the existence of any double bond (C(17)=C(18) in **3·OTf** exhibits a 1.405(3) Å bond distance). The Ir-C(17) bond distance (2.133(2) Å) is shorter than both Ir-C carbon distances of η^2-coordinated COE ligand in **3·OTf** and slightly longer than those reported for the related [IrH(κ^3-*N,N´,N´´*-Tp)(σ-cyclooctenyl)(COE)] species (2.058 and 2.051(11) Å).[21]

Conclusions

The reactivity of ^{Me}Tpm with the dinuclear iridium(I) precursors [Ir(μ-Cl)(COE)$_2$]$_2$ and [Ir(μ-Cl)(COD)]$_2$ has been investigated. Both reactions afford the mononuclear complex [IrCl(κ^1-*N*-^{Me}Tpm)(COD)] (**1**). The κ^1-*N* ligation mode of the ^{Me}Tpm ligand to iridium(I) in **1** has been unambiguously confirmed by X-ray diffraction methods. The formation of **1** from the reaction of [Ir(μ-Cl)(COE)$_2$]$_2$ with ^{Me}Tpm has been rationalized by an iridium-promoted transfer dehydrogenation process. Moreover, a mechanism for this transformation, comprising both the dehydrogenation and hydrogenation of COE, has been proposed based on theoretical calculations at the DFT level and on NMR studies. The calculations have shown that the oxidative addition of the unactivated C^5-H bond of COE ligand to iridium is favoured over the activation of the allylic C^3-H bonds.

Reactivity studies has allowed the isolation and characterization of Ir-^{Me}Tpm organometallic complexes with the ^{Me}Tpm ligand in κ^1-*N*, κ^2-*N,N´* or κ^3-*N,N´,N´´* ligation mode. Finally, this sequential reactivity studies have led the synthesis of a rare Ir-^{Me}Tpm complex featuring hydride, carbonyl and σ-cyclooctyl ligands, which has been fully characterized in solution and in the solid state by X-ray diffraction methods.

Experimental

General Information

All manipulations were performed with rigorous exclusion of air at an argon/vacuum manifold using standard Schlenk-tube techniques or in a dry-box (MB-UNILAB). Solvents were dried by the usual procedures and distilled under argon prior to use or taken under argon from a Solvent Purification System (SPS). The starting materials [Ir(μ-Cl)(COE)$_2$]$_2$,[22] [Ir(μ-Cl)(COD)]$_2$[23] and the ^{Me}Tpm[24] ligand were prepared according to methods reported in the literature.

NMR spectra were recorded on a Varian Gemini 2000, a Bruker ARX 300, a Bruker Avance 300 MHz or a Bruker Avance 400 MHz instrument. Chemical shifts (expressed in parts per million) are referenced to residual solvent peaks (^{1}H, ^{13}C{^{1}H}). Coupling constants, *J*, are given in Hertz. C, H, and N analyses were carried out in a Perkin-Elmer2400 CHNS/O analyzer. Mass spectroscopy was measured on an Esquire 3000+ with Ion trap detector interfaced to an Agilent 1100 series HPLC system.

Reaction of ^{Me}Tpm with [Ir(μ-Cl)(COE)]$_2$ in C$_6$D$_6$

A mixture of [Ir(μ-Cl)(COE)$_2$]$_2$ (0.050 g, 0.056 mmol) and ^{Me}Tpm (0.034 g, 0.112 mmol) was prepared under argon in a NMR tube

and then dissolved in C_6D_6 (0.4 mL). The resulting sample was place in a DrySyn NMR heating block for NMR tubes, heated at 353 K and periodically studied by NMR spectroscopy.

Synthesis of [IrCl(κ^1-^{Me}Tpm)(COD)] (1)

A mixture of $[Ir(\mu\text{-}Cl)(COD)]_2$ (0.70 g, 1.04 mmol) and ^{Me}Tpm (0.62 g, 2.08 mmol) in toluene (15 mL) was stirred at room temperature until it forms a clear red solution (about 2 h). The solution was concentrated in vacuo to 2.0 mL and pentane (10 mL) was added to yield a bright yellow precipitate. Greenish yellow single crystals suitable for X-ray analysis were obtained from a concentrated benzene solution of **1**. Yield: 0.950 g (72 %). Anal. calcd. for $C_{24}H_{34}ClIrN_6$ (634.2): C, 45.45; H, 5.40; N, 13.35. Found: C, 45.42; H, 5.57; N, 12.91. Mass spectrometry (Maldi$^+$): m/z 619.4 (M^+ - H + CH_3). ^{1}H NMR (CD_2Cl_2, 300 MHz, 193 K): δ 9.15 (s, 1H, *H*C$_{N3}$), 6.07 (s, 1H, pz-C*H*), 6.03 (s, 1H, pz-C*H*), 5.88 (s, 1H, pz-C*H*), 4.33 (br, 1H, cod-C*H*), 4.20 (br, 1H, cod-C*H*), 2.95 (b, 1H, cod-C*H*), 2.63 (s, 3H, pz-C*H*$_3$), 2.45 (s, 3H, pz-C*H*$_3$), 2.16 (s, 3H, pz-C*H*$_3$), 2.07-2.04 (br, 6H, pz-C*H*$_3$ + 1H, cod-C*H*), 1.64 (s, 3H, pz-C*H*$_3$), 0.94-1.54 (m, 8 H, cod-C*H*$_2$). ^{13}C{^{1}H} NMR (CD_2Cl_2, 75.5 MHz, 193 K): 10.5, 10.9, 11.0, 13.5, 13.7, 15.4 (all s, pz-*C*H$_3$), 29.5, 31.1, 31.4, 32.5 (all s, cod-*C*H$_2$), 57.6, 61.5, 69.3, 70.6 (all s, cod-*C*H), 78.6 (s, H*C*$_{N3}$), 106.7, 107.8, 109.3 (all s, pz-*C*H), 140.7, 141.0, 144.6, 148.2, 147.5, 150.0 (all s, pz-*C*$_{quart}$). IR (cm^{-1}): 1560 (ν$_{C=N}$).

Synthesis of [Ir(κ^2-^{Me}Tpm)(COD)]OTf (2·OTf)

A mixture of **1** (0.13 g, 0.20 mmol) and AgOTf (0.05 g, 0.20 mmol) in dichloromethane (10 mL) was stirred in the dark at room temperature for 2 h. The reaction mixture was filtered through tight Celite pack and the resulting solution was concentrated in vacuo to 2.0 mL. The addition of pentane (10 mL) allowed the precipitation of orange solid which was dried in vacuo. Single crystals suitable for X-ray analysis were obtained from layering concentrated dichloromethane solutions of **2.OTf** with pentane. Yield: 0.11 g (74 %). Anal. calcd. for $C_{25}H_{34}F_3IrN_6O_3S$ (747.85): C, 40.15; H, 4.58; N, 11.24. Found: C, 39.81; H, 4.55; N, 11.08. Mass spectrometry (Maldi$^+$): m/z 619.36 (M^+ - (CF_3SO_3 + H + CH_3). ^{1}H NMR (CD_2Cl_2, 300 MHz, 294 K): δ 7.83 (s, 1H, *H*C$_{N3}$), 6.19 (s, 3H, pz-C*H*), 4.12 (br, 4H, cod-C*H*), 2.40 (s, 9H, pz-C*H*$_3$), 2.31 (s, 9H, pz-C*H*$_3$), 2.01 (b, 4H, cod-C*H*$_2$), 1.52 (br, 4H, cod-*C*H$_2$). ^{13}C{^{1}H} NMR (CD_2Cl_2, 75.5 MHz, 294 K): 11.9, 15.1 (both s, pz-*C*H$_3$), 39.9 (s, cod-*C*H$_2$) 65.8 (s, cod-*C*H), 74.9 (s, H*C*$_{N3}$), 111.1 (s, pz-*C*H), 144.3, 154.6 (both s, pz-*C*$_{quart}$). ^{19}F{^{1}H}NMR (CD_2Cl_2, 75.5 MHz, 294 K): - 78.92 (s). IR (cm^{-1}): 1561 (ν$_{C=N}$).

Synthesis of [IrH$_2$(κ^3-^{Me}Tpm)(COE)]OTf (3·OTf)

In a thick wall teflon stoppered glass tube, a mixture of $[Ir(\mu\text{-}Cl)(COE)_2]_2$ (0.375 g, 0.42 mmol), ^{Me}Tpm (0.250 g, 0.84 mmol) and NaOTf (0.144 g, 0.84 mmol) was suspended in dichloromethane (15 mL) and degassed by freeze-thaw method. The tube was pressurized with H_2 (1 bar) and stirred at room temperature for 30 mins. The colour of the suspension faded to near colourless. Solvent was completely removed under vacuum and the residue washed with pentane (2 x 5 mL) and then redissolved in dichloromethane (5 mL) and filtered through Celite. Subsequent concentration and addition of pentane afforded a white solid. Single crystals for X-ray analysis were obtained from slow cooling of concentrated benzene solutions of **3·OTf**. Yield: 0.580 g (92 %). Anal. calcd. for $C_{25}H_{38}F_3IrN_6O_3S$ (751.88): C, 39.94; H, 5.09; N, 11.18. Found: C, 40.40; H, 5.23; N, 11.05. Mass spectrometry (Maldi$^+$): m/z 603.28 (M^+ - CF_3SO_3) ^{1}H NMR (CD_2Cl_2, 300 MHz, 294 K): δ 7.81 (s, 1H, *H*C$_{N3}$), 6.17 (br s, 2H, pz-C*H*), 6.06 (s 1H, pz-C*H*), 4.12 (m, 2H, COE-C*H*), 2.66 (s, 6H, pz-C*H*$_3$), 2.52 (s, 3H, pz-C*H*$_3$), 2.45-2.36 (m, 2H, COE-C*H*), 2.29 (s, 6H, pz-C*H*$_3$), 2.18 (s, 3H, pz-C*H*$_3$), 1.96 – 1.35 (m, 4H, COE-C*H*$_2$), -22.83 (s, 2H, Ir-H). ^{13}C{^{1}H} NMR (CD_2Cl_2, 75.5 MHz, 294 K): 11.6, 11.7, 15.5, 17.3 (all s, pz-*C*H$_3$), 26.9, 32.9, 33.2 (all s, COE-*C*H$_2$), 62.7 (s, COE-*C*H), 70.6 (s, H*C*$_{N3}$), 110.1 (s, pz-*C*H), 143.4, 156.9 (both s, pz-*C*$_{quart}$). ^{19}F{^{1}H}NMR (CD_2Cl_2, 75.5 MHz, 294 K): - 78.97 (s). IR (cm^{-1}): 2190 (s), 2227 (w) both (ν$_{Ir\text{-}H}$), 1567 (ν$_{C=N}$).

Synthesis of [IrH(cyclooctyl)(CO)(κ^3-^{Me}Tpm)]OTf (4·OTf).

In a thick wall teflon stoppered glass tube, compound **3·OTf** (0.2 g, 0.27 mmol) was dissolved in dichloromethane (10 mL) and degassed by freeze-thaw method. The tube was pressurized with 2 bar of CO and heated at 323 K for 3 days to give a pale reddish yellow solution. The solvent was completely removed under vacuum and the solid residue washed with pentane (2 x 5 mL), and extracted with dichloromethane (8 mL). Subsequent concentration of the solution in vacuo to 2.0 mL and addition of pentane (10 mL) afforded a colourless solid. Single crystals suitable for X-ray analysis were obtained by layering dichloromethane solutions of **4·OTf** with pentane. Yield: 0.180 g (85 %). Anal. calcd. for $C_{26}H_{38}F_3IrN_6O_4S$ (779.89): C, 40.04; H, 4.91; N, 10.78. Found: C, 39.75; H, 4.93; N, 10.81. Mass spectrometry (Maldi$^+$): m/z 631.27 (M^+ - CF_3SO_3). ^{1}H NMR (CD_2Cl_2, 300 MHz, 294 K): δ 7.91 (s, 1H, *H*C$_{N3}$), 6.26 (s, 2H, pz-C*H*), 6.07 (s 1H, pz-C*H*), 3.35 (m, 1H, cot-C*H*)), 2.70 (s, 3H, pz-C*H*$_3$), 2.68 (s, 3H, pz-C*H*$_3$), 2.57 (s, 6H, pz-C*H*$_3$), 2.55 (s, 3H, pz-C*H*$_3$), 2.21 (s, 3H, pz-C*H*$_3$), 1.88 – 1.26 (m, 14H, cot-C*H*$_2$), -18.05 (s, 1H, Ir-H). ^{13}C{^{1}H} NMR (CD_2Cl_2, 75.5 MHz, 294 K): 9.8 (s, cot-*C*H), 11.5, 11.6, 11.9, 15.2, 15.3, 16.8 (all s, pz-*C*H$_3$), 26.6, 27.1, 27.2, 28.5, 29.7 (all s, cot-*C*H$_2$), 40.6, 42.6 (both s, cot-*C*H$_2$ adjacent to –*C*H), 70.3 (s, H*C*$_{N3}$), 108.5, 109.9, 110.1 (s, pz-*C*H), 142.4, 143.1, 144.4, 154.4, 155.4, 157.0 (all s, pz-*C*$_{quart}$), 168.1 (s, Ir-CO). ^{19}F{^{1}H}NMR (CD_2Cl_2, 75.5 MHz, 294 K): - 78.94 (s). IR (cm^{-1}): 2196 (ν$_{Ir\text{-}H}$), 2020 (ν$_{Ir\text{-}CO}$).

Reaction of [Ir(COD)(κ^2-^{Me}Tpm)]OTf (2·OTF) with H_2

This reaction was performed both in a Young NMR tube and at preparative scale in a pressure tube. (a) Young NMR tube experiment: A CD_2Cl_2 solution (0.6 mL) of **2.OTF** (0.04 g, 0.053 mmol) prepared in a Young NMR tube was pressurized with H_2 (1 bar) after three cycles of freeze thawing and heated at 323 K. The reaction was monitored by ^{1}H-NMR spectroscopy and after three days the NMR tube was recharged with H_2 (1 bar) and heated at 323 K overnight which resulted in the completion of the reaction; (b) Preparative scale: A pressure tube was charged with a CD_2Cl_2 solution (10 mL) of **2·OTF** (0.200 g, 0.27 mmol) and

pressurized with H_2 (2 bar). The reaction mixture was heated at 323K for three days. The Solvent was completely removed in vacuo, and the residue washed with pentane (twice), and extracted with dichloromethane (10 mL). The CH_2Cl_2 solution was concentrated to c.a. 1 mL and precipitated with pentane to afford a white powder which was characterized as complex **3·OTF**. In both experiments, it was observed that a black precipitate was formed from the first day. The colour of the solutions was intense yellow.

Monitoring of the reaction of $[Ir(\mu\text{-}Cl)(COE)_2]_2$ with ^{Me}Tpm. A Young NMR tube was charged with $[Ir(\mu\text{-}Cl)(COE)_2]_2$ (15 mg, 0.017 mmol), ^{Me}Tpm (10 mg, 0.034 mmol) and C_6D_6 (0.8 mL). The NMR tube was closed under argon and heated at 353K. The resulting solution was periodically monitored by ^{1}H NMR.

Structure determination of compounds 1, 2·OTf, 3·OTf and 4·OTf

X-ray diffraction data were collected at 100(2)K with graphite-monochromated Mo Kα radiation (λ = 0.71073 Å) using narrow ω rotations (0.3°) on a Bruker APEX DUO diffractometer. Intensities were integrated and corrected for absorption effects with SAINT-PLUS[25] and SADABS[26] programs, included in APEX2 package. The structure was solved by direct methods with SHELXS-2013[27] and refined by full-matrix least-squares refinement on F2 with SHELXL-2014[28] included in WinGX.[29] CCDC 1812901-1812904 contains the supplementary crystallographic data for this paper. These data can be obtained free of charge from The Cambridge Crystallographic Data Centre via www.ccdc.cam.ac.uk/structures.

Crystal data compound 1. $C_{24}H_{34}ClIrN_6$, M = 634.22; yellow prism 0.090 x 0.179 x 0.191 mm^3; triclinic *P-1*, a = 7.5778(3), b = 10.4101(4), c = 30.6151(12) Å, α=90.5790(10), β=95.3880(10), γ=90.4360(10), V = 2404.21(16) Å^3; Z = 4; T = 100(2) K; D_c = 1.752 g/cm^3; μ = 5.689 mm^{-1}; 25483/12204 reflections measured/unique (R_{int} = 0.0221), number of data/restraint /parameters 12204/0/649, final *GoF* = 1.065, $R_1(F^2)$ = 0.0240 (11060 reflections, $I > 2\sigma(I)$) and w$R(F^2)$ = 0.0563 (all data).

Crystal data compound 2·OTf. $C_{24}H_{34}IrN_6{\cdot}CF_3O_3S$, M = 747.84; orange prism 0.091 x 0.106 x 0.153 mm^3; monoclinic $P2_1/n$, a = 8.5533(3), b = 13.9441(5), c = 22.6818(9) Å, β=96.3320(10), V = 2688.71(17) Å^3; Z = 4; T = 100(2) K; D_c = 1.847 g/cm^3; μ = 5.104 mm^{-1}; 29413/7084 reflections measured/unique (R_{int} = 0.0236), number of data/restraint /parameters 7084/1/421, final *GoF* = 1.050, $R_1(F^2)$ = 0.0188 (6414 reflections, $I > 2\sigma(I)$) and w$R(F^2)$ = 0.0453 (all data).

Crystal data compound 3·OTf. $C_{24}H_{38}IrN_6{\cdot}CF_3O_3S{\cdot}C_6D_6$, M = 836.02; colourless plate 0.083 x 0.140 x 0.230 mm^3; triclinic *P-1*, a = 11.4694(5), b = 11.6677(5), c = 13.9878(6) Å, α=92.3850(10), β=103.8370(10), γ = 111.5710(10), V = 1672.77(13) Å^3; Z = 2; T = 100(2) K; D_c = 1.660 g/cm^3; μ = 4.111 mm^{-1}; 32584/8693 reflections measured/unique (R_{int} = 0.0290), number of data/restraint/parameters 8693/2/462, final *GoF* = 1.044, $R_1(F^2)$ = 0.0192 (8200 reflections, $I > 2\sigma(I)$) and w$R(F^2)$ = 0.0457 (all data). Hydride ligands positions have been calculated with potential minimization calculus with HYDEX program and refined with a restraint in Ir-H bond lengths.

Crystal data compound 4·OTf. $C_{25}H_{38}IrN_6O{\cdot}CF_3O_3S$, M = 779.88; white prism 0.085 x 0.103 x 0.231 mm^3; triclinic *P-1*, a = 8.2713(3), b = 9.7845(4), c = 19.0733(7) Å, α=75.6490(10), β=85.0880(10), γ = 79.8680(10), V = 1470.69(10) Å^3; Z = 2; T = 100(2) K; D_c = 1.761 g/cm^3; μ = 4.672 mm^{-1}; 17642/7487 reflections measured/unique (R_{int} = 0.0172), number of data/restraint/parameters 7487/1/456, final *GoF* = 1.079, $R_1(F^2)$ = 0.0190 (7264 reflections, $I > 2\sigma(I)$) and w$R(F^2)$ = 0.0472 (all data). Hydride ligand has been included in observed position and freely refined.

Computational Details

All DFT theoretical calculations were carried out using the Gaussian program package.[30] The B3LYP method,[31] including the D3 dispersion correction scheme developed by Grimme[32] with Becke Johnson damping, has been used for both energies and gradient calculations. All atoms were treated with the def2-SVP basis set[33] together with the corresponding core potential for Ir for geometry optimizations. Energies were further refined by single point calculations using the def2-TZVP basis set. The "ultrafine" grid was employed in all calculations. All reported energies are Gibbs free energies referred to a 1 atm standard state at 298.15 K removing the contribution to the translational entropy, as indicated by Morokuma et al.[34] The nature of the stationary points was confirmed by analytical frequency analysis, and transition states were characterized by a single imaginary frequency corresponding to the expected motion of the atoms.

Conflicts of interest

"There are no conflicts to declare".

Acknowledgements

Financial support from MINECO/FEDER under the projects CTQ2015-67366-P and CTQ2016-75884-P and DGA/FSE (group E07) is gratefully acknowledged. Dr. P. García-Orduña acknowledges CSIC, European Social Fund and Ministerio de Economía y Competitividad of Spain for a PTA contract. Dr. R. Lalrempuia acknowledges support from ARAID foundation.

Notes and references

1 (a) I. Alkorta, R. M. Claramunt, E. Díez-Barra, J. Elguero, A. de la Hoz, C. López, *Coord. Chem. Rev.* 2017, **339**, 153-182; (b) J.-E. Park, S. K. Kang, J. O. Woo, K.-s. Son, *Dalton Trans*, 2015, **44**, 9964-9969; (c) L. M. D. R. S. Martins, A. J. L. Pombeiro, *Coord. Chem. Rev.*, 2014, **265**, 74-88; (d) A. Otero, J. Fernández-Baeza, A. Lara-Sánchez, L. F. Sánchez-Barba, *Coord. Chem. Rev.*, 2013, **257**, 1806-1868; (e) L. G. Lavrenova, A. D. Strekalova, A. V. Virovets, D. A. Piryazev, V. A. Daletskii, L. A.

Sheludyakova, T. F. Mikhailovskaya, S. F. Vasilevskii, *Rus. J. Coord. Chem.,* 2012, **38**, 507-514; (f) J. Zhang, A. Li, T. S. A. Hor, *Organometallics*, 2009, **28**, 2935-2937; (g) C. Pettinari, R. Pettinari, *Coord. Chem. Rev.,* 2005, **249**, 525-543; (h) C. Pettinari, R. Pettinari, *Coord. Chem. Rev.,* 2005, **249**, 663-691; (g) H. R. Bigmore, S. C. Lawrence, P. Mountford, C. S. Tredget, *Dalton Trans.*, 2005, 635-651; (i) A. Sánchez-Méndez, G. F. Silvestri, E. de Jesús, F. J. de la Mata, J. C. Flores, R. Gómez, P. Gómez-Sal, *Eur. J. Inorg. Chem.*, 2004, 3287-3296; (j) D. L. Reger, T. C. Grattan, K. J. Brown. C. A. Little, J. J. S. Lamba, A. L. Rheingold, R. D. Sommer, *J. Organomet. Chem.* 2000, **607**, 120-128; (k) I. K. Dhawan, M. A. Bruck, B. Schilling, C. Grittini, J. H. Enemark, *Inorg. Chem.* 1995, **34**, 3801-3808; (l) S. Trofimenko, *J. Am. Chem. Soc.*, 1970, **92**, 5118-5126.

2 (a) B. A. McKeown, J. P. Lee, J. Mei, T. R. Cundari, T. B. Gunnoe, *Eur. J. Inorg. Chem.,* 2016, 2296–2311; (b) M. Paneque, M. L. Poveda, N. Rendón, *Eur. J. Inorg. Chem.,* 2011, 19–33; (c) S. Conejero, M. Paneque, M. L. Poveda, L. L. Santos, E. Carmona, *Acc. Chem. Res.* 2010, **43**, 572–580; (d) C. Slugovc, I. Padilla-Martínez, S. Sirol, E. Carmona, *Coord. Chem. Rev.,* 2001, **213**, 129-157; (e) S. Trofimenko, *Chem. Rev.,* 1993, **93**, 943-980.

3 (a) R. Lalrempuia, A. Stasch, C. Jones, *Chem. Asian. J*. 2015, **10**, 447-454; (b) S. González-Gallardo, I. Kuzu, P. Oña-Burgos, T. Wolfer, C. Wang, K. W. Klinkhammer, W. Klopper, S. Bräse, F. Breher, *Organometallics,* 2014*,* **33**, 941-951*;* (c) F. Breher, J. Grunenberg, S. C. Lawrence, P. Mountford, H. Rüegger, *Angew. Chem. Int. Ed.* 2004, **43**, 2521-2524.

4 I. Krummenacher, H. Rüegger, F. Breher, *Dalton Trans.*, 2006, 1073-1081.

5 (a) M. Paneque, S. Sirol, M. Trujillo, E. Gütiérrez-Puebla, M. A. Monge, E. Carmona, *Angew. Chem. Int. Ed.* 2000, **39**, 218-221; (b) M. Paneque, S. Sirol, M. Trujillo, E. Carmona, E. Gütiérrez-Puebla, M. A. Monge, C. Ruiz, F. Malbosc, C. Serra-Le Berre, P. Kalck, M. Etienne, J. C. Daran, *Chem. Eur. J.,* 2001, **7**, 3868-3879.

6 (a) M. Hernández-Juárez, V. Salazar, E. V. García-Báez, I. I. Padilla-Martínez, H. Höpfl, M. J. Rosales-Hoz, *Organometallics,* 2012, **31**, 5438-5451; (b) A. J. Hallett, K. M. Anderson, N. G. Connelly, M. F. Haddow, *Dalton Trans.*, 2009, 4181-4189; (c) I. I. Padilla-Martínez, M. L. Poveda, E. Carmona, M. A. Monge, C. Ruiz-Valero, *Organometallics*, 2002, **21**, 93-104; (d) D. M. Heinekey, W. J. Jr. Oldham, J. S. Wiley, *J. Am. Chem. Soc.,* 1996, **118**, 12842-12843; (e) M. A. Esteruelas, L. A. Oro, R. M. Claramunt, C. López, J. L. Lavandera, J. Elguero, *J. Organomet. Chem.,* 1989, **366**, 245-255; (f) M. A. Esteruelas, L. A. Oro, M. C. Apreda, C. Foces-Foces, F. H. Cano, R. M. Claramunt, C. Lopez, J. Elguero, M. Begtrup, *J. Organomet. Chem.,* 1988, **344**, 93-108.

7 ^{1}H NMR (C_6D_6, 300 MHz, 298 K): δ 1.50 (s, 16H, COA), ^{13}C{^{1}H} NMR plus APT and ^{1}H-^{13}C HSQC (C_6D_6, 75 MHz, 298 K): δ 27.0 (s, COA).

8 C. Gemel, R. John, C. Slugovc, K. Mereiter, R. Schmid, K. Kirchner, *J. Chem. Soc., Dalton Trans*., 2000, 2607-2612.

9 F. Malbosc, P. Kalck, J.-C. Daran, M. Etienne, *J. Chem. Soc., Dalton Trans.*, 1999, 271-272.

10 For recent papers and reviews see: (a) R. B. Leveson-Gower, P. B. Webb, D. B. Cordes, A. M. Z. Slawin, D. M. Smith, R. P Tooze, J. Liu, Organometallics, 2018, **37**, 30–39; (b) A. Kumar, T. M. Bhatti, A. S. Goldman, *Chem. Rev.*, 2017, **117**, 12357-12384; (c) J. Choi, A. H. R. MacArthur, M. Brookhart, A. S. Goldman, *Chem. Rev.*, 2011, **111**, 1761-1779.

11 (a) R. H. Crabtree, J. A. Mihelcic, J. M. Quirk, *J. Am. Chem. Soc.*, 1979, **101**, 7738-7740; (b) W. H. Bernskoetter, E. Lobkovsky, P. J. Chirik, *Organometallics,* 2005, **24**, 6250-6259; (c) J. S. Siegel, K. K. Baldridge, A. Linden, R. Dorta, *J. Am. Chem. Soc.*, 2006, **128**, 10644-10645; (d) S. A. Hauser, R. Tonner, A. B. Chaplin, *Organometallics,* 2015, **34**, 4419-4427.

12 O. O. Kovalenko, O. Wendt, *Dalton Trans.,* 2016, **45**, 15963-15969.

13 (a) M. Martín, O. Torres, E. Oñate, E. Sola, L. A. Oro, *J. Am. Chem. Soc.,* 2005, **127**, 18074-18084; (b) M. Martín, E. Sola. O. Torres, P. Plou, L. A. Oro, *Organometallics,* 2003, **22**, 5406-5417.

14 R. H. Crabtree, M. F. Mellea, J. A. Mihelcic, J. M. Quirk, *J. Am. Chem. Soc.*, 1982, **104**, 107-113.

15 D. H. Nguyen, J. J. Pérez-Torrente, M. V. Jiménez, F. J. Modrego, D. Gómez-Bautista, F. J. Lahoz, L. A. Oro, *Organometallics,* 2013, **32**, 6918-6930.

16 S. Azpeitia, U. Prieto, E. San Sebastián, A. Rodríguez-Diéguez, M. Garralda, M. A. Huertos, *Dalton Trans*, 2018, **47**, 6808-6818.

17 C. J. Adams, N. G. Connelly, D. J. H. Emslie, O. D. Hayward, T. Manson, A. G. Orpen, P. H. Rieger, *Dalton Trans*., 2003, 2835-2845.

18 R. Lalrempuia, M. Iglesias, V. Polo, P. J. Sanz Miguel, F. J. Fernández-Alvarez, J. J. Pérez-Torrente, L. A. Oro, *Angew. Chem. Int. Ed*., 2012, **51**, 12824-12827.

19 I. Göttker-Schnetmann, M. Brookhart, *J. Am. Chem. Soc.* 2004, **126**, 9330-9338.

20 F. M. Alías, P. J. Daff, M. Paneque, M. L. Poveda, E. Carmona, P. J. Pérez, V. Salazar, Y. Alvarado, R. Atencio, R. Sánchez-Delgado, *Chem. Eur. J.,* 2002, **8**, 5132-5146.

21 M. J. Fernández, M. J. Rodriguez, L. A. Oro, F. J. Lahoz, *J. Chem. Soc. Dalton Trans.* **1989**, 2073-2076.

22 A. Van der Ent, A. L. Onderdelinden, *Inorg. Synth.,* 1973, **14**, 92-95.

23 J. L. Herde, J. C. Lambert, C. V. Senuff, M. A. Cushing, *Inorg. Synth.,* 1974, **15**, 18-20.

24 R. M. Claramunt, C. López, C. Jaime, A. Virgili, C. Marco, J. Elguero, *Heterocycles,* 1995, **40**, 175-186.

25 SAINT+, version 6.01: Area-Detector Integration Software, Bruker AXS, Madison, WI, 2001.

26 (a) R. H. Blessing, *Acta Cryst*., 1995, **A51**, 33-38; (b) SADABS, Area Detector Absorption Correction Program, Bruker AXS, Madison, WI, 1996.

27 G. M. Sheldrick, *Acta Cryst*., 1990, **A46**, 467-473.

28 G. M. Sheldrick, *Acta Cryst*., 2008, **A64**, 112-122.

29 L. J. Farrugia, *J. Appl. Cryst*., 2012, **45**, 849-854.

30 Gaussian 09, Revision D.01, M. J. Frisch, G. W. Trucks, H. B. Schlegel, G. E. Scuseria, M. A. Robb, J. R. Cheeseman, G. Scalmani, V. Barone, G. A. Petersson, H. Nakatsuji, X. Li, M. Caricato, A. Marenich, J. Bloino, B. G. Janesko, R. Gomperts, B. Mennucci, H. P. Hratchian, J. V. Ortiz, A. F. Izmaylov, J. L. Sonnenberg, D. Williams-Young, F. Ding, F. Lipparini, F. Egidi, J. Goings, B. Peng, A. Petrone, T. Henderson, D. Ranasinghe, V. G. Zakrzewski, J. Gao, N. Rega, G. Zheng, W. Liang, M. Hada, M. Ehara, K. Toyota, R. Fukuda, J. Hasegawa, M. Ishida, T. Nakajima, Y. Honda, O. Kitao, H. Nakai, T. Vreven, K. Throssell, J. A. Jr. Montgomery, J. E. Peralta, F. Ogliaro, M. Bearpark, J. J. Heyd, E. Brothers, K. N. Kudin, V. N. Staroverov, T. Keith, R. Kobayashi, J. Normand, K. Raghavachari, A. Rendell, J. C. Burant, S. S. Iyengar, J. Tomasi, M. Cossi, J. M. Millam, M. Klene, C. Adamo, R. Cammi, J. W. Ochterski, R. L. Martin, K. Morokuma, O. Farkas, J. B. Foresman, D. J. Fox, Gaussian, Inc., Wallingford CT, 2016.

31 (a) C. Lee, W. Yang, R. G. Parr, *Phys. Rev. B,* 1988, **37**, 785–789; (b) A. D. Becke, *J. Chem. Phys.* 1993, **98**, 1372–1377; (c) A. D. Becke, *J. Chem. Phys.,* 1993, **98**, 5648–5652.

32 S. Grimme, J. Antony, S. Ehrlich, H. Krieg, *J. Chem. Phys.,* 2010, **132**, 154104.

33 F. Weigend, R. Ahlrichs, *Phys. Chem. Chem. Phys.,* 2005, **7**, 3297–3305.

34 R. Tanaka, M. Yamashita, L. W. Chung, K. Morokuma, K. Nozaki, *Organometallics*, 2011, **30**, 6742–6750.